Impurity-induced polaritons in a one-dimensional chain

Alexey Yamilov

Department of Physics, Queens College of City University of New York, Flushing, New York 11367

Lev I. Deych

Department of Physics, Seton Hall University, 400 South Orange Avenue, South Orange, New Jersey 07079

Alexander A. Lisyansky

Department of Physics, Queens College of City University of New York, Flushing, New York 11367

Received February 2, 2000; revised manuscript received May 19, 2000

A detailed analytical study of an impurity-induced polariton band arising inside a spectral gap between lower and upper polariton branches is presented. Using the microcanonical method, we calculate the density of states and the localization length of the impurity polaritons. Analytical results are compared with numerical simulations, and excellent agreement is found. © 2000 Optical Society of America [S0740-3224(00)00709-8]

OCIS codes: 160.4760, 160.6000, 260.0260.

1. INTRODUCTION

The opportunity to create Anderson localized states of electromagnetic excitations in disordered dielectrics has attracted a great deal of attention during the past two decades.[1,2] Although the localization of light in three-dimensional (3D) uniform-on-average random systems proved difficult to achieve, new opportunities opened up with the development of structures with periodically modulated dielectric properties, the so-called photonic crystals.[3,4] It was first suggested in Ref. 5 that the photon localization could be more easily achieved if the photon density of states (DOS) were depleted at certain frequency domains. Photonic crystals allow the creation of photon bandgaps, regions of frequencies in which the photon DOS is zero. Introducing isolated defects in such structures, one can create local photon modes similar to well-known defect phonon modes in regular crystals[6–10] or electron impurity states in semiconductors.[11] A forbidden gap in the photonic spectrum occurs when the electromagnetic wavelength becomes comparable with the lattice constant. Consequently, for microwave, infrared, and visible ranges, the photonic crystal is a structure of macroscopic dimensions. Local states in these structures also arise owing to defects of macroscopic dimensions. The great interest in photonic crystals is promoted by their highly unusual quantum electrodynamic properties. For instance, spontaneous emission, which is completely suppressed within the frequency range of the bandgaps,[12] can be effectively controlled by introduction of local modes.[13,14]

The intriguing possibilities of photonic crystals initiated interest in optical effects in other types of photonic bandgaps. Such gaps can arise, for example, between different polariton branches. The fact that the frequency region between polariton branches can represent a stop band for electromagnetic waves propagating in certain directions has been well known for a long time. The reflection coefficient in this situation can reach a magnitude of 90% or greater. This effect was used in the 1940's and 1950's to create monochromatic infrared beams (it was called the method of residual or reststrahlen rays, and the respective spectral interval was called the reststrahlen region). However, in certain cases the stop bands exist for all the directions, and then a genuine spectral gap arises with the same consequences for quantum electrodynamics as in the case of photonic crystals. This was first realized in Ref. 15, in which it was shown that a two-level atom can form an atom-field coupled states with suppressed emission similar to the states discussed in Ref. 16 for photonic crystals. Periodic arrangement of such two-level systems produces an impurity-induced polariton band within the polariton gap.[17]

Local polariton states associated with a regular isotopic defect without any intrinsic optical activity were introduced in Refs. 18 and 19. These states are coupled states of electromagnetic excitations with phonons (or excitons), with both components, including the electromagnetic component, being localized in the vicinity of the defect. These states are, in a certain sense, analogous to local photons in photonic crystals considered in Refs. 13 and 14, although they arise owing to microscopic impurities in regular crystal lattices. On the other hand, local polaritons can be considered as local excitations of a crystal coupled with the electromagnetic field. Regular local phonons (excitons) also interact with the electromagnetic field, but this interaction results mainly in absorption of light and radiative decay of the states.[10] The local polaritons arise in the region where electromagnetic waves

do not propagate, and there are, therefore, neither defect-induced absorption of light nor radiative damping of the local states. The electromagnetic interaction leads in this case to new optical effects and strongly affects the properties of the local states. It is well known, for instance, that local phonons or excitons in a 3D system (as well as local photons in photonic crystals) arise only if the strength of a defect exceeds a certain threshold. Local polaritons in systems with an isotropic dispersion split off the allowed band without a threshold even in three dimensions.[18] This effect is caused by the interaction with electromagnetic field, which results in the Van–Hove singularity in the polariton DOS.

A different type of localized electromagnetic excitation interacting with dipole active media was considered in Refs. 20 and 21. In these papers, dipole optical excitations in highly disordered fractal structures were considered. Localization in this case is achieved because of the highly disordered fractal nature of the structures rather than because of depletion of the electromagnetic density of states in some frequency interval. Since we do not consider fractal structures in this paper, local polaritons in what follows are understood as excitations arising inside spectral gaps of a host structure.

One of the optical effects caused by local polaritons is resonant tunneling of the electromagnetic wave with gap frequencies. This effect was first suggested in Ref. 22, in which the results of numerical simulation of electromagnetic wave propagation through a relatively short one-dimensional (1D) chain with a single defect were reported. It was found that the transmission coefficient at the frequency of the local polariton state increases dramatically up to a value close to unity. In spite of the general understanding that local states should produce local tunneling, this result still seems surprising because transmission of light is effected by a defect with microscopic dimensions much smaller than the light's wavelength. In addition, the energy of the electromagnetic component of local polaritons is much smaller than that of the phonon component. Traditional wisdom based upon properties of conventional propagating polaritons tells us that, in such a situation, most of the incident radiation must be simply reflected. The results of Ref. 22 demonstrated that this logic does not apply to local polaritons. The physical explanation of the result can be given on the basis of consideration of local polaritons as the result of interaction between the electromagnetic field and local phonons. The latter have macroscopic dimensions comparable with light's wavelength, making the interaction effective. An electromagnetic wave is carried through a sample by phonons, which is tunneling resonantly owing to the local state with mostly phonon contribution. Tunneling was confirmed in Refs. 23 and 24, in which we analytically calculated the transmission coefficient through a linear chain with a single defect. We found that a light impurity indeed gives rise to the resonance transmission through the forbidden gap of the polariton spectrum. The resonance occurs when the defect is placed at the center of the chain. The transmission at the resonance becomes independent of the chain's length and reaches the value of unity if the resonance frequency coincides with the center of the polariton gap. The analytical calculations provided an explanation for the numerical results of Ref. 22; in particular it explained a strongly asymmetrical frequency profile of the transmission coefficient and the presence of a deep minimum following directly after the maximum.

The 1D model with one or many impurities used in Refs. 22–24 was meant to provide an insight into optical properties of 3D dielectrics with pointlike defects. In spite of their obvious limitations, 1D models proved to be a useful tool for studying dynamics of dielectrics and were used extensively in the past to obtain frequencies of local and extended optical phonons, which agreed reasonably well with experiments (see, for instance, reviews on dielectric properties of mixed crystals in Ref. 25). In a sense, the model considered in this paper is a version of the widely used, so-called random-element isodisplacement models.[25] The model is applied, however, to a new situation, when a local frequency, associated with the impurity, falls in the reststrahlen region of the host crystal.

At the same time, the same model of the chain of discrete noninteracting pointlike dipoles coupled with the retarded electromagnetic field can also be considered in a different context. It can be shown that this model describes normal propagation of light through a system of multiple quantum wells (MQW's), which were studied in a number of theoretical and experimental papers.[26–32] The local state considered in Refs. 22–24 in this context corresponds to an interface mode, which is localized only in the growth direction of the MQW structure but is extended in the in-plane directions. The idea of a local polariton state in a periodic MQW structure was first put forward in Ref. 33, in which the dispersion equations for local states with different polarizations were obtained for a general model of a defect layer. The presence of interface modes in various multilayered system is not new. These modes arise and are well studied in ideal periodic structures; see for instance, Refs. 34 and 35 and references therein. What distinguishes the interface mode, which arises in MQW owing to the presence of a defect layer, is that its in-plane wave vector $k_{\parallel}$ can be equal to zero, whereas localized interface modes in ideal periodic multilayers exist only for $k_{\parallel} > \omega/c$, where ω is the frequency and c is the speed of light in the respective background medium. Therefore this local mode can be excited by an evanescent electromagnetic mode at normal incidence and may cause its resonant transmission. An application of the results obtained in Refs. 22–24 to MQW structures is of significant experimental interest and deserves a detailed discussion, which will be published elsewhere.

The main purpose of this paper is to present the results of analytical study of the properties of the impurity-induced band, which grows from our local polariton state when the concentration of the impurities increases. This band was first considered in Ref. 24, which describes numerical simulations of the electromagnetic wave transmission through the chain with a finite concentration of impurities. Neglecting spatial dispersion of phonons, we are able to obtain analytical expressions for DOS and the Lyapunov exponent (LE) for the band in the limit of a large concentration of impurities $l_0/l_{\mathrm{def}} \gg 1$, where l_{def} is the average distance between impurities and l_0 is the lo-

calization length of the single local polariton state. In this limit the method of microcanonical ensemble, complemented by expansion over $(l_0/l_{\mathrm{def}})^{-1}$, gives the DOS of an effective system with a uniform distribution of impurities and describes its renormalization caused by local fluctuations of impurity positions. It also reveals localization of the states of the band, which are all localized owing to the 1D nature of the model. The properties of this polariton band are found to be drastically different from that of the band produced by two-level atoms.[17] The analytical results show excellent agreement with numerical calculations and lead to suggestions regarding experimental observation of the impurity-induced polariton bands. In the context of MQW structures the results of this paper describe normal propagation of electromagnetic waves through a system containing two types of quantum wells (QW) stacked together at random.

2. MODEL OF ONE-DIMENSIONAL POLARITONS AND THE METHOD OF CALCULATIONS

A. Model

The main objective of this paper is to study properties of the impurity-induced polariton band arising within the polariton gap of a 1D chain of atoms with dipole moments P_n, where n refers to a position of an atom in the chain. We assume that atoms of the chain do not directly interact with each other and are coupled only by a retarded electromagnetic field. This assumption means neglect of a spatial dispersion of material excitations of the chain, which is usually a good assumption for optical phonons. In the case of MQW interpretation of the model this assumption means the absence of direct interactions between excitons of different wells, which is also good, provided that the wells are not too close to each other. Dynamics of the chain interacting with electromagnetic field $E(x)$ is then described by a simple equation:

$$(\Omega_n^2 - \omega^2)P_n = \alpha E(x_n), \tag{1}$$

where α is a coupling parameter between the dipoles and the electromagnetic field and Ω_n^2 represents a site energy. We shall assume that the chain is composed of atoms of two different types, which differ in their site energy only. In this case, Ω_n^2 can be presented in the following form:

$$\Omega_n^2 = \Omega_0^2 + \Delta\Omega^2 c_n, \tag{2}$$

where $\Delta\Omega^2 = \Omega_1^2 - \Omega_0^2$, Ω_0^2, and Ω_1^2 are site energies of the respective atoms and c_n is a random variable that takes values 0 and 1 with probabilities $1 - p$ and p, respectively. We assume that $p \ll 1$ so that Ω_0 is attributed to host atoms, whereas Ω_1 corresponds to the impurities. Equation (1) can be interpreted in terms of both excitonlike and phononlike excitations. In the latter case, $\Delta\Omega^2 = (1 - M_{\mathrm{imp}}/M_{\mathrm{host}})\omega^2$, where M_{host} and M_{imp} are the masses of host atoms and impurities, respectively.

Polaritons in the system arise as collective excitations of dipoles (polarization waves) coupled to the electromagnetic wave, $E(x_n)$. The equation of motion of the electromagnetic component is given by the Maxwell equation:

$$\frac{\omega^2}{c^2}E(x) + \frac{\mathrm{d}^2E}{\mathrm{d}x^2} = -4\pi\frac{\omega^2}{c^2}\sum_n P_n\delta(na - x), \tag{3}$$

where c is the speed of the electromagnetic wave in vacuum and a is the distance between two nearest-neighbor dipoles. This equation actually describes only the TE field, and we assume that no coupling to other polarizations occurs. In Ref. 36 a chain of quantum dots interacting with an electromagnetic field was considered. This interaction resulted in a short-range quasi-static dipole–dipole interaction and a long-range retarded interaction between the dots. Our model reproduces only retarded part of the interaction, since there is no longitudinal fields in our model. This situation corresponds to transverse vibrations in isotropic three-dimensional crystals and to T-polarized polaritons in the case of MQW's. Equations (1) and (3) present a microscopic description of the transverse electromagnetic waves propagating along the chain in the sense that the description takes into account all modes of the field including those with wave numbers outside of the first Brillouin band. Within the chosen model, these equations fully describe electromagnetic interaction between the dipoles with retardation exactly taken into account. The microscopic nature of our approach is particularly important for consideration of MQW's, since the interatomic distance in the latter case can be of the order of magnitude of the electromagnetic wavelength, and consideration of short-wave components of the electromagnetic field is crucial.

Considering propagation of the electromagnetic wave as a sequence of scattering events separated by free propagation, one can present Eq. (3) in a discrete form. The entire system of dynamic equations (1) and (3) can then be transformed into a transfer-matrix form:

$$v_{n+1} = \hat{\tau}_n v_n, \tag{4}$$

Vectors v_n with components $(E_n, E_n'/k)$, where E_n and E_n' are the electromagnetic field and its derivative at the nth site, represent the state of the system, and the transfer matrix $\hat{\tau}_n$ is a 2×2 matrix of the following form:

$$\hat{\tau}_n = \begin{bmatrix} \cos ka & \sin ka \\ -\sin ka + \beta_n(ka)\cos ka & \cos ka + \beta_n(ka)\sin ka \end{bmatrix}. \tag{5}$$

The parameter β_n is given by

$$\beta_n = \frac{d^2}{\omega^2 - \Omega_n^2}, \tag{6}$$

with $d^2 = 4\pi\alpha/a$ representing the polarizability of the nth dipole. The transfer matrix of this form is equivalent to the transfer matrix describing propagation of light in QW structures.[26–28]

In the case of a single impurity an approximate equation for the frequency of the local state was first derived in Ref. 33 for a defect of a general form. In the particular case of a defect atom that is different from hosts by its resonance frequency Ω_1 only, the following equation for the frequency of the local state was derived in Refs. 23 and 24:

$$\omega_{\mathrm{loc}}^2 = \Omega_1^2 - d^2 \frac{\omega_{\mathrm{loc}} a}{2c} \frac{\Delta\Omega^2}{\sqrt{(\omega_{\mathrm{loc}}^2 - \Omega_0^2)(\Omega_0^2 + d^2 - \omega_{\mathrm{loc}}^2)}}, \tag{7}$$

which is exact in the long-wave limit $a\omega/c \ll 1$. The last term here describes the shift of the local frequency from the resonance frequency Ω_1 of the impurity owing to coupling to the electromagnetic field; $\Delta\Omega^2 = \Omega_1^2 - \Omega_0^2$ is the measure of the difference between host atoms and the impurity. In the case of the atomic interpretation of the model this radiative shift is very small, but taking into account the direct interaction between the atoms (the spatial dispersion of atomic excitations) moves the local frequency farther away from Ω_1. However, this formula can also be applied to short-period MQW's. In this case the radiative shift described by Eq. (7) can be made large enough and observed experimentally. The transmission coefficient through the chain passes through the maximum at ω_{loc} and goes to zero at Ω_1.[23,24] For experimental observation of this effect it is sufficient to have the radiative shift greater than homogeneous broadening of the QW exciton resonance at Ω_1.

The main object of interest in this paper is the properties of the impurity-induced band in the case of a finite concentration of impurities. They are characterized by the Lyapunov exponent (LE), λ, which in our case can be defined as[37]

$$\lambda = \lim_{L\to\infty} \frac{1}{L} \ln \frac{\|\Pi_1^N \hat{\tau}_n v_0\|}{\|v_0\|}, \tag{8}$$

where L is the total length of the chain consisting of N atoms. It is well known that the quantity defined by Eq. (8) is nonrandom (self-averages). It characterizes the spatial extent of the envelope of system eigenstates, all of which are localized in one dimension (see Ref. 38 and references therein). The same quantity also describes the typical value of the transmission coefficient, T, of an external excitation incident upon the system: $T_{\mathrm{typ}} \simeq \exp(-\lambda L)$, and through the Thouless relation[39] it determines the DOS of the system. Calculation of the LE in the spectral region of the polariton gap of the pure system is the main task of this subsection.

B. Method of Microcanonical Ensemble

The major problem with calculation of the LE or the DOS in the region of impurity bands is that a simple concentration expansion is not able to describe the impurity band. Electron and phonon impurity bands have been intensively studied in the past (see, for example, Ref. 38). In the limit of extremely small concentration of impurities, $(pl_0)/a \ll 1$, it was proved possible to provide a regular systematics of the arising states and to use statistical arguments to describe their DOS.[6] Another method used for this type of calculations employed the so-called phase formalism (see Ref. 38 and references therein). This approach allowed one to calculate the DOS of impurity bands in different spectral regions, including exponential behavior at the tails of the band for both small and large, $(pl_0)/a \gg 1$, concentrations. In the case of local polaritons the localization length, l_0, of an individual local state can be so large that one has to deal with the situation described by the latter inequality even in the case of a rather small concentration of impurities. Therefore in this paper we focus mainly on the properties of the well-developed polariton impurity band when individual local states are overlapped. To this end we use the method of the microcanonical ensemble, which was first suggested for analytical calculations of the LE in 1D single-band model of a disordered alloy.[37] The advantage of this method over other methods of DOS calculations is that it allows one to calculate simultaneously both the DOS and the localization length. Its main shortcoming is, as we shall see below, that this method is a version of effective-media methods, and as such it is unable to describe the DOS near fluctuation boundaries of the spectrum. At the same time the results obtained allow a clear physical interpretation and, as follows from comparison with numerical simulations, they quite accurately describe properties of the bulk of the impurity band.

The starting point of our calculations is the general definition of the LE given by Eq. (8). In spite of the LE being a self-averaging quantity, it is convenient in practical calculations to perform averaging over the random configurations of the impurities. The regular ensemble of the realization is described by the fixed concentration of the impurities p, and their total number can vary from realization to realization. Therefore one can distinguish two causes for fluctuations: (1) local arrangements of the impurities and (2) the total number of the impurities. The main idea of the method of microcanonical ensemble is to reduce the finite size fluctuations in the system, eliminating the fluctuations of the total number of impurities. Such an ensemble with a fixed number of impurities is called the microcanonical ensemble in analogy with statistical physics. At the same time the result of the averaging in the limit $L\to\infty$ should not depend on the type of ensemble used by virtue of the self-averaging nature of the LE. The key idea of the microcanonical method is based on the assumption that with one cause of fluctuations eliminated, one can obtain reliable results when the microcanonical ensemble average of $\langle \ln(...)\rangle$ is replaced by $\ln\langle ...\rangle$. Such a substitution gives an exact result in the case of commutating matrices and leads to an excellent agreement between analytical calculations and simulations in the case of 2×2 matrices with a single-band spectrum.[37]

Using the microcanonical ensemble, one can evaluate the average over all matrix sequences using the following expression derived in Ref. 37:

$$\left\langle \prod_1^N \hat{\tau}_n \right\rangle = \binom{N}{pN}^{-1} \frac{1}{(pN)!} \frac{\partial^{pN}}{\partial x^{pN}} (\hat{\tau}_0 + x\hat{\tau}_1)^N \Big|_{x=0}, \tag{9}$$

where $\hat{\tau}_0$ and $\hat{\tau}_1$ are host and defect matrices, respectively, and x a free parameter. The derivative in Eq. (9) then can be presented in the form of the Cauchy integral

$$\left\langle \prod_1^N \hat{\tau}_n \right\rangle = \binom{N}{pN}^{-1} \frac{1}{2\pi i} \int_C \mathrm{d}x \frac{\nu^N(x)}{x^{pN+1}} \hat{D}(x), \tag{10}$$

where the contour of integration C is taken on the complex plane around $x = 0$, $\nu(x)$ is the largest eigenvalue of the matrix $\hat{\tau}_0 + x\hat{\tau}_1$, and the matrix $\hat{D}(x)$,

$$\hat{D}(x) = \nu^{-N}(x)(\hat{\tau}_0 + x\hat{\tau}_1)^N, \tag{11}$$

has eigenvalues not exceeding 1 in absolute value. In the limit of large N the above integral can be evaluated by the saddle-point method. As the result we arrive at the following expression for the complex-valued LE, $\tilde{\lambda}$:

$$\tilde{\lambda} = \lim_{N\to\infty} \frac{1}{L} \ln\left[\text{largest eigenvalue} \left\langle \prod_1^N \hat{\tau}_n \right\rangle \right]$$

$$= \frac{1}{a}[\ln \nu(x_0) - (1-p)\ln x_0 + p \ln p + (1-p)\ln(1-p)], \tag{12}$$

where x_0 is defined by the saddle-point equation

$$\left.\frac{\partial \ln \nu(x)}{\partial \ln x}\right|_{x=x_0} = p. \tag{13}$$

The real part of $\tilde{\lambda}$ given by Eq. (12) represents LE, while its imaginary part according to Thouless[39] gives the integral density of states $N(\omega)$ in the impure system:

$$\lambda = \mathrm{Re}[\tilde{\lambda}], \tag{14}$$

$$N(\omega) = -\frac{1}{\pi}\mathrm{Im}[\tilde{\lambda}]. \tag{15}$$

The eigenvalues of the matrix $\hat{\tau}_0 + x\hat{\tau}_1$ can be found from the equation

$$\frac{\nu}{1+x} + \frac{1+x}{\nu} = \kappa(x) = 2\cos(ka) + \frac{\beta_0 + x\beta_1}{1+x}, \tag{16}$$

where β_0 and β_1 are polarizabilities of the host and the defect atoms, respectively.

It is convenient to rewrite Eqs. (12) and (16) in terms of a new variable $y = x/(1+x)$:

$$\kappa(y) = (1-y)\nu(y) + \frac{1}{(1-y)\nu(y)} = \kappa_0(\omega) + yF(\omega), \tag{17}$$

$$\kappa_0(\omega) = 2\cos(ka) + d^2 ka \sin(ka)\frac{1}{\omega^2 - \Omega_0^2}, \tag{18}$$

$$F(\omega) = d^2 ka \sin(ka)\frac{\Omega_1^2 - \Omega_0^2}{(\omega^2 - \Omega_0^2)(\omega^2 - \Omega_1^2)}. \tag{19}$$

In the long-wave limit $\epsilon = ka \ll 1$, functions $F(\omega)$ and $\kappa_0(\omega)$ can be simplified and presented in the form that clarifies their physical meaning:

$$F(\omega) \simeq \epsilon^2 f(\omega),$$

$$\kappa_0(\omega) \simeq 2 + \epsilon^2 \gamma(\omega),$$

where $f(\omega)$ is defined according to

$$f(\omega) \simeq \frac{d^2(\Omega_1^2 - \Omega_0^2)}{(\omega^2 - \Omega_0^2)(\omega^2 - \Omega_1^2)} \tag{20}$$

and represents the difference $\beta_1 - \beta_0$ between polarizabilities (6) of the impurities and host atoms. Function $\gamma(\omega)$, defined as

$$\gamma(\omega) = 1 + \frac{d^2}{\Omega_0^2 - \omega^2}, \tag{21}$$

is the long-wave dielectric function of the pure chain.

Similarly, Eq. (12) transforms into

$$\tilde{\lambda}(p) = \ln\{[1 - y_0(p)]\nu[y_0(p)]\} - \left[p \ln\frac{y_0(p)}{p} + (1-p)\ln\frac{1-y_0(p)}{1-p}\right], \tag{22}$$

with the saddle-point equation reading as

$$\pm \frac{y(1-y)F}{\sqrt{(\kappa_0 + yF)^2 - 4}} + y\Bigg|_{y=y_0} = p. \tag{23}$$

The choice of the sign in Eq. (23) is determined by the requirement to use the greatest of the eigenvalues ν. Introduction of the new variable y turns $\kappa(y)$ in a linear function of y, essentially simplifying future calculations.

3. LYAPUNOV EXPONENT AND THE DENSITY OF STATES

A. Boundaries of the Impurity Band

Dielectric function $\gamma(\omega)$ determines the frequency region of the polariton gap: for $\Omega_0^2 < \omega^2 < \Omega_0^2 + d^2$ it is negative, and hence, propagating modes do not exist in this region. We shall assume that the defect frequency Ω_1^2 obeys the inequality $\Omega_0^2 < \Omega_1^2 < \Omega_0^2 + d^2$, so that the impurity-induced band develops inside the gap of the original spectrum. As we already mentioned, the approach we use in the paper belongs to the class of effective-medium approximations since we neglect here certain kinds of fluctuations in the system. Therefore it is natural to expect that within this approach the impurity band would have well-defined spectral boundaries, outside of which the differential DOS remains exact zero. Our first goal is to determine these boundaries and find the concentration dependence of the width of the impurity band. The differential DOS, $\rho(\omega) = \mathrm{d}N(\omega)/\mathrm{d}\omega$, takes on nonzero values when $\tilde{\lambda}(\omega)$ acquires a nonconstant imaginary part. Rewriting Eq. (22) in the form

$$\tilde{\lambda}(\omega) = \frac{1}{a}\left(\ln\left\{\frac{1}{2}\left[\kappa_0 + y_0 F \pm \frac{y_0(1-y_0)F}{p - y_0}\right]\right\} - \left[p\ln\frac{y_0}{p} + (1-p)\ln\frac{1-y_0}{1-p}\right]\right), \tag{24}$$

one can see that in the case of real y_0, $\mathrm{Im}\,\tilde{\lambda}(\omega)$ can be either zero or π (the latter happens when the argument of ln is negative). In both cases differential DOS is obviously zero, and it can only take on a nonzero value when y_0 becomes complex. Equation (23), which defines y_0, is formed by a polynomial of the third order with real coefficients; therefore it has either three real roots or one real solution and a complex-conjugated pair. In order to describe formation of the polariton band, one has to select the root, which has a complex component in a certain frequency interval and yields a positive LE. Comparison with numerical simulations shows that the choice of only one of three saddle points, according to the above-

mentioned criteria, produces the correct description of the impurity band. It is not difficult to show that at the frequency at which $y_0(\omega)$ becomes complex, the derivative $\partial y_0/\partial\omega$ diverges. This fact gives us an explicit equation for the spectrum boundaries. From Eq. (23) one can find that the divergence occurs when y_0 satisfies the equation

$$y_0^3F[F(1-p)+\kappa_0]+y_0^2[\kappa_0F(1-3p)+k_0^2-4] + y_0\kappa_0(F-2\kappa_0^2+4)+p(\kappa_0^2-4)=0. \quad (25)$$

Equations (23) and (25) define the concentration dependence of the boundaries of the polariton impurity band. An approximate solution of this equation can be obtained as a formal series in powers of parameter $\epsilon = ka$. However, it will be seen from the results that the actual expansion parameter in this case is $1/pl_0 \ll 1$. The solution of Eq. (23) with the accuracy to ϵ^2 can be obtained in the form

$$y = p - p(1-p)\frac{f}{2\sqrt{pf-\gamma}}\epsilon + p(1-p) \times \frac{2(pf-\gamma)f(1-2p)-fp(1-p)}{8(pf-\gamma)^2}f^2\epsilon^2, \quad (26)$$

where $y = p$ is the only nonvanishing zero-order approximation for y. Since two other solutions, $y = 0$, correspond to a singular point of the integral (10), the chosen solution $y = p$ represents the only saddle point accessible within our perturbation scheme. Using additional criteria outlined above, we verify that the solution given by Eq. (26) correctly reproduces the behavior of the LE. Substituting Eq. (26) into Eq. (22), one finds the complex LE in the long-wavelength approximation:

$$\tilde{\lambda}(\omega) = \frac{\omega}{c}\left\{\sqrt{pf(\omega)-\gamma(\omega)} - \frac{p(1-p)f^2(\omega)}{8[pf(\omega)-\gamma(\omega)]}\epsilon\right\}. \quad (27)$$

According to Eq. (27), $\tilde{\lambda}(\omega)$ acquires an imaginary part at frequencies obeying the inequality

$$pf(\omega)-\gamma(\omega) \leqslant 0. \quad (28)$$

The boundaries are determined by the respective equation $pf(\omega)-\gamma(\omega)=0$, which coincides with the long-wavelength limit of Eq. (25). This equation determines two points at which $pf(\omega)-\gamma(\omega)$ changes sign to negative:

$$\omega_{\mathrm{il}}^2 = \frac{(\Omega_0^2+\Omega_1^2+d^2)-\sqrt{(\Omega_0^2+d^2-\Omega_1^2)^2+4d^2(\Omega_1^2-\Omega_0^2)p}}{2},$$

$$\omega_{\mathrm{pu}}^2 = \frac{(\Omega_0^2+\Omega_1^2+d^2)+\sqrt{(\Omega_0^2+d^2-\Omega_1^2)^2+4d^2(\Omega_1^2-\Omega_0^2)p}}{2}, \quad (29)$$

The first of these solutions belongs to the initial polariton bandgap and as such represents the low-frequency boundary of the new impurity band. The second one lies outside of the gap and is a bottom frequency, modified by impurities, of the upper polariton branch of the initial spectrum. These two frequencies, however, are not the only points at which the expression $pf(\omega)-\gamma(\omega)$ turns negative. Two other points are

$$\omega_{pl}^2 = \Omega_0^2,$$
$$\Omega_{iu}^2 = \Omega_1^2, \quad (30)$$

and the change of the sign at these points occurs through infinity of $pf(\omega)-\gamma(\omega)$ rather than through zero. These two frequencies do not depend on the concentration of impurities and therefore present stable genuine boundaries of the spectrum. This property of Ω_0 and Ω_1 is due to their resonance nature (they correspond to the poles of the respective polarizabilities) and disappears when, for example, the spatial dispersion is taken into account. At the same time, the numerical simulations of Ref. 24, in which the spatial dispersion was taken into consideration, indicate that the shift of these frequency from their initial values is negligibly small for realistic values of the interatom interaction parameter Φ, even for a relatively large concentration of impurities.

These four frequencies set the modified boundaries of the initial polariton spectrum of the pure system (ω_{pl}^2, ω_{pu}^2), and boundaries of the newly formed impurity band (ω_{iu}^2, ω_{il}^2). The lower boundary of the forbidden gap of the crystal, Ω_0, is not affected by the impurities; the singularity in the polariton DOS at this point survives for any concentrations of defects. The upper boundary of the bandgap, ω_{pu}, shifts toward higher frequencies with the concentration, and when $p = 1$, it coincides with the upper band boundary of the new crystal, $\Omega_L^i = (\Omega_1^2 + d^2)^{1/2}$. Frequencies ω_{il} and ω_{iu} give approximate values for the lower and the upper boundaries of the impurity-induced pass band that arises inside the original forbidden gap $\Omega_0 < \omega_{\mathrm{il}} < \omega_{\mathrm{iu}} < (\Omega_0^2 + d^2)^{1/2}$. The impurity band grows asymmetrically with concentration: while its lower boundary moves toward Ω_0 with an increase of the concentration, the upper edge remains fixed at $\omega_{\mathrm{iu}} = \Omega_1$. Such a behavior of the impurity band agrees well with our numerical results.[24]

The width of the impurity-induced band defined in terms of squared frequencies $\Delta_{\mathrm{im}}^2 = \omega_{\mathrm{iu}}^2 - \omega_{\mathrm{il}}^2$ can be found from Eqs. (29) and (30) as

$$\Delta_{\mathrm{im}}^2 = \frac{\sqrt{(\Omega_0^2+d^2-\Omega_1^2)^2+4d^2(\Omega_1^2-\Omega_0^2)p}-(\Omega_0^2+d^2-\Omega_1^2)}{2}. \quad (31)$$

For Ω_1 not very close to the upper boundary of the initial polariton gap, $\Omega_L = (\Omega_0^2 + d^2)^{1/2}$, the linear in p approximation is sufficient to describe the concentration dependence of the bandwidth

$$\Delta_{\mathrm{im}}^2 \approx \frac{d^2(\Omega_1^2-\Omega_0^2)p}{\Omega_0^2+d^2-\Omega_1^2}. \quad (32)$$

When Ω_1, however, happens to be close to Ω_L, a crossover is possible from the linear dependence (32) of the square-root behavior:

$$\Delta_{\mathrm{im}}^2 \approx \sqrt{d^2(\Omega_1^2-\Omega_0^2)p}. \quad (33)$$

The condition for such crossover to occur is

$$1 \ll p \ll \frac{(\Omega_0^2 + d^2 - \Omega_1^2)^2}{4d^2(\Omega_1^2 - \Omega_0^2)}.$$

B. Lyapunov Exponent and the Density of States Far from the Spectrum Boundaries

Using Eqs. (14), (15), and (27), one can calculate the LE and the integral DOS for different regions of the spectrum. For allowed bands, $(0, \Omega_0)$, $(\omega_{\mathrm{il}}, \Omega_1)$, and $(\omega_{\mathrm{pu}}, \infty)$, one has

$$\lambda(\omega) = -\frac{p(1-p)f^2}{8(pf-\gamma)}\frac{\omega}{c}\epsilon + O(\epsilon^2),$$

$$N(\omega) = \frac{1}{\pi}\frac{\omega}{c}\sqrt{|pf-\gamma|} + O(\epsilon^2); \tag{34}$$

for forbidden bands, $(\Omega_0, \omega_{\mathrm{il}})$ and $(\Omega_1, \omega_{\mathrm{pu}})$, we obtain

$$\lambda(\omega) = \frac{\omega}{c}\left\{\sqrt{pf-\gamma} - \left[\frac{p(1-p)f^2}{8(pf-\gamma)}\right]\epsilon\right\},$$

$$N(\omega) = 0. \tag{35}$$

One can see from Eqs. (34) and (35) that within allowed bands the DOS appears in the zero order of the formal expansion parameter ϵ, whereas the LE starts from the first order. For the forbidden bands the situation is reversed: the LE contains a term of zero order in ϵ, whereas the DOS in this order disappears. This observation suggests a simple physical interpretation of the microcanonical approximation in conjunction with the expansion over ϵ. Analysis of the series in this parameter shows that the actual small parameter is $a/(pl_0) = l_{\mathrm{def}}/l_0$, where l_{def} is a mean distance between impurities. The zero-order expansion in this parameter can be interpreted as a uniform continuous ($l_{\mathrm{def}} \to 0$) distribution of impurities with concentration p. The results in this approximation then correspond to the polariton impurity band that would exist in such a uniform system. The parameter l_{def}/l_0 in this case is a measure of disorder in the distribution of impurities, which leads to the localization of excitations described by the DOS in Eq. (34) with the localization length, $l^{-1} = \lambda$, presented in the first line of the same equation.

Let us now consider frequencies in the interval $\omega \in (0, \Omega_0) \cup (\Omega_L^i, \infty)$, where passbands of the pure chains composed of either host or impurity atoms overlap. The DOS in this region can be written in a physically transparent form,

$$N(\omega) = \sqrt{(1-p)N_0^2(\omega) + pN_1^2(\omega)}, \tag{36}$$

where $N_0(\omega)$ and $N_1(\omega)$ are an integral DOS in pure chains containing host atoms or impurities, respectively. In the remaining portion of the initial spectrum, $\omega \in (\omega_{\mathrm{up}}, \Omega_L^i)$ (but not very close to the boundary ω_{up}, where the expansion ceases to be valid), DOS can be presented as $N(\omega) = [(1-p)N_0^2(\omega) - pl_1^2(\omega)]^{1/2}$, where l_1 is the penetration length through the polariton gap of the 100% impure chain.

Our main goal, however, is obtaining the DOS and the LE of the impurity-induced band, $\omega \in (\omega_{\mathrm{il}}, \Omega_1)$. Near the center of this region the DOS can be presented in the following form:

$$N(\omega) = \frac{1}{\pi l_0}\left\{1 + \frac{4|\gamma|\omega_c}{pd^2}(\omega - \omega_c) + O\left[\left(\frac{\omega-\omega_c}{d}\right)^2\right]\right\}, \tag{37}$$

where ω_c is the center of the impurity band, which in the linear in p approximation is

$$\omega_c^2 = \Omega_1^2 - \frac{1}{2}\Delta_{\mathrm{im}}^2, \tag{38}$$

where Δ_{im}^2 is the width of the band in terms of squared frequencies defined in Eq. (32). The first term in Eq. (37) represents the total number of states between ω_{il} and the center of the band; it is interesting to note that this number does not depend on concentration of impurities. The coefficient at the second term gives the differential DOS at the center and can be rewritten as

$$\rho(\omega_c) = \frac{4|\gamma|\omega_c}{\pi l_0 pd^2} = \frac{2}{\pi l_0 \delta}, \tag{39}$$

where $\delta = \Delta_{\mathrm{im}}^2/2\omega_c$ is an approximate expression for the impurity band width $\delta \simeq \Omega_1 - \omega_{\mathrm{il}}$. This DOS has a simple meaning of the average density of states uniformly distributed through the entire band over the distance equal to $l_0/2$. In 1D uniform systems the wave number of the respective excitations, k, is simply connected to $N(\omega)$: $k = \pi N(\omega)$. The differential DOS would in this case be proportional to the inverse group velocity. Accordingly, $1/\pi\rho(\omega_c)$ given by Eq. (39) can also be viewed as a group velocity, v, of excitations in the center of our impurity band in the case of the uniform distribution of impurities. The expression for v can also be presented as

$$v = \frac{d^2}{4\pi_c^2|\gamma|^{3/2}}pc \ll c, \tag{40}$$

which demonstrates that polariton excitations of the impurity band have much slower velocities not only compared with c but also with the velocities at both regular polariton branches.

Expanding Eq. (34) for the LE about the center of the band, we obtain a parabolic frequency dependence of the localization length of the impurity polaritons:

$$l(\omega) = \lambda(\omega)^{-1} = 2l_0(pl_0)\left[1 - \frac{20\gamma^2}{p^2}\left(\frac{\omega^2-\omega_c^2}{d^2}\right)^2\right]. \tag{41}$$

One can see from this expression that $l(\omega)$ reaches its maximum value $2pl_0^2$ at the center of the band. It is important to note that the localization length here grows linearly with the concentration, whereas it is the LE that grows with the concentration for frequencies outside of the impurity band. An increase of the concentration of the impurities also results in fast ($\propto 1/p^2$) flattening of the maximum in the localization length, the fact we first noticed in our numerical simulations.[24]

The frequency dependence of the LE, defined by Eqs. (22) and (23), is shown in Fig. 1. For frequencies corre-

sponding to the impurity band the LE drops sharply (the localization length increases); it then diverges at the upper boundary of the impurity band. This divergence has the same origin as the LE divergence at the lower boundary of the bandgap of the original crystal, where, owing to the specificity of the polariton spectrum, the wave vector becomes infinite. The concentration dependence of the LE and the integral DOS for some frequency $\omega_0 \in (\Omega_0, \Omega_1)$ is shown in Fig. 2. For $p = 0$ this frequency belongs to the forbidden gap; thus DOS is zero. With an increase of the concentration the LE decreases (the localization length increases). For the concentration when the lower boundary of the impurity band crosses ω_0 the DOS becomes nonzero, and in $\lambda(\omega)$ the crossover between behaviors described by Eqs. (35) and (34) occurs. In Fig. 3 we compare the results of our analytical calculations with numerical simulations of Ref. 24. The comparison shows an excellent agreement between numerical and analytical results, confirming the validity of the microcanonical method in the considered limit. In addition, since numerical results were obtained with the spatial dispersion taken into account, the comparison shows that the model with dispersionless phonons produces reliable results for the LE even not very far away from the spectrum boundaries.

C. Solution in the Vicinity of the Spectrum Boundary: Nonanalytical Behavior

The results obtained in the previous subsection are clearly not valid for frequencies close to the band boundaries ω_{il} and ω_{pu}, where $pf - \gamma = 0$ and the second term in expansion (26) diverges. It is well known that perturbation expansions in disordered systems usually fail in the vicinity of boundaries of the initial spectrum of the system unperturbed by disorder.[38] The regions in the vicinity of these special frequencies ω_{il} and ω_{pu} require special consideration. Attempting to regularize our ϵ expansion, we shall seek corrections to the zero-order solution in the form

$$y = p + B\epsilon^{\alpha}, \tag{42}$$

admitting a possibility of fractional values of α and hence nonanalytical behavior of the solution. We also introduce a new variable ζ that determines the proximity to either of two frequencies ω_{il} or ω_{pu}:

$$pf - \gamma = \zeta\epsilon^{\alpha'}. \tag{43}$$

Substituting these expressions into Eq. (23) and equating the lowest-order terms, we see that the equation can only be satisfied for $\alpha = \alpha' = 2/3$. In this case we find that the parameter B introduced in Eq. (42) obeys the equation

$$\frac{p(1-p)f}{2\sqrt{\zeta + Bf}} + B = 0. \tag{44}$$

The substitution of y given by Eq. (42) in the condition for the spectral boundaries presented by Eq. (25) allows one to obtain an exact expression for the renormalized boundary

$$pf - \gamma = \left[3p^{2/3}(1-p)^{2/3}\left(\frac{-f}{2}\right)^{4/3}\right]\epsilon^{2/3}, \tag{45}$$

that modifies Eq. (28). The shift is small by virtue of smallness of $\epsilon^{2/3}$. In the lowest order in ϵ the new positions of the band edges for small p are

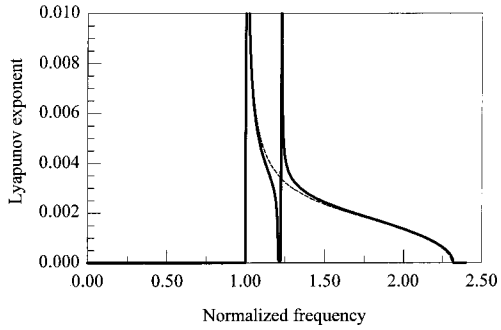

Fig. 1. LE for a chain with a defect concentration of 10% (solid curve) in comparison with a pure system (dashed curve).

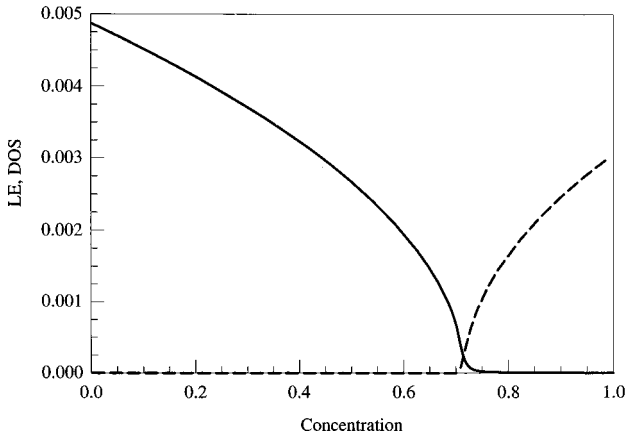

Fig. 2. Dependences of LE (solid curve) and DOS (dashed curve) on concentration for a frequency in the interval $\Omega_0 < \omega < \Omega_1$.

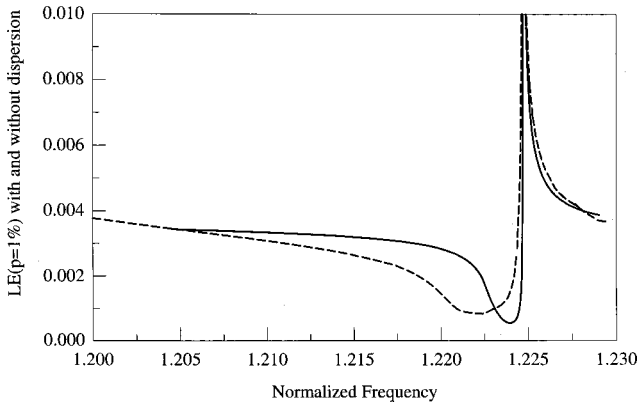

Fig. 3. Comparison of LE calculated both with (dashed curve) and without (solid curve) spatial dispersion in the vicinity of Ω_1. The concentration of defects for both curves is 1%.

$$\tilde{\omega}_{\mathrm{il}}^2 = \Omega_1^2 - \frac{d^2(\Omega_1^2 - \Omega_0^2)}{d^2 - (\Omega_1^2 - \Omega_0^2)} p\left[1 + 3\left(\frac{a}{4pl_0}\right)^{2/3}\right],$$

$$\tilde{\omega}_{\mathrm{pu}}^2 = \Omega_L^2 + \frac{d^2(\Omega_1^2 - \Omega_0^2)}{d^2 - (\Omega_1^2 - \Omega_0^2)} p\left[1 - 3\left(\frac{a}{16pl_0}\right)^{1/3}\right], \tag{46}$$

where we again encounter $a/(pl_0)$ as a true small parameter of the expansion. It is interesting to note the different character of nonanalytical corrections to the positions of the boundary of the impurity band $\tilde{\omega}_{\mathrm{il}}^2$ and the bottom of the upper polariton branch $\tilde{\omega}_{\mathrm{pu}}^2$. They have fractional concentration dependence with the correction to $\tilde{\omega}_{\mathrm{pu}}^2$ being much stronger in the limit $a/(pl_0) \ll 1$.

Now let us consider the modification of the LE and the integral DOS owing to the nonanalyticity. Substituting Eq. (42) into Eq. (22), the complex LE can be written as

$$\tilde{\lambda} = -\frac{p(1-p)f}{2B}\epsilon^{4/3} = \sqrt{(pf - \gamma) + Bf\epsilon^{2/3}}\epsilon. \tag{47}$$

This expression explicitly demonstrates the crossover between analytical and nonanalytical behavior. When frequency ω lies far from the initial boundary $|pf - \gamma| \gg Bf\epsilon^{2/3}$, one recovers the term proportional to ϵ with the same coefficient as in Eq. (27), whereas in the opposite limit $|pf - \gamma| \ll Af\epsilon^{2/3}$, when we approach the boundary, the leading term gains fractional power and becomes $\propto \epsilon^{4/3}$.

At the vicinity of the renormalized spectral boundary, Eq. (46), DOS $\rho(\omega) \equiv 0$ to the left of $\tilde{\omega}_{\mathrm{il}}$, and for $\omega > \tilde{\omega}_{\mathrm{il}}$ it can be obtained as

$$\rho(\omega) = \frac{3}{\pi d}\left(\frac{\gamma}{l_0}\right)^{1/2} \frac{1}{(l_0 p)^{1/2}} \frac{\omega}{(\omega^2 - \tilde{\omega}_{\mathrm{il}}^2)^{1/2}}, \tag{48}$$

where γ and l_0 are evaluated at $\omega = \Omega_1$, and we have neglected the renormalization of the boundary when calculating the coefficient in $\rho(\omega)$. In this approximation the frequency and the concentration dependence of the DOS does not change as compared with the one obtained from nonrenormalized expansion (34). However, it is interesting that the renormalization brings about an additional numerical factor of 3 in Eq. (48), which is absent in the nonrenormalized expression. This frequency dependence is typical for excitations with the quadratic dispersion law in the long-wave approximation. The main characteristic of this dispersion law is the effective mass m, which can be found from Eq. (48) as

$$m = \frac{9\gamma}{2pd^2 l_0^2} = \frac{9\gamma^2}{2pc^2}\left(\frac{\omega_{\mathrm{il}}}{d}\right)^2. \tag{49}$$

It is interesting to compare this expression with the effective mass of the upper polariton branch of the pure system at the bottom of the band $2m_0 = (\omega_L/dc)^2$. The two expressions have a similar structure if one introduces a renormalized speed of light,

$$\tilde{c} = c\sqrt{p/9\gamma^2}. \tag{50}$$

Although the introduced parameter $\tilde{c}$ does not have a direct meaning of the speed of the excitations, it shows again that the excitations in the impurity polariton band are considerably slower than their regular counterparts, with a similar dispersion law at the spectrum boundary as well as at the center of the band. However, unlike the center-of-band situation (40) the renormalized velocity at the edge is proportional to the square root of concentration.

The LE in the vicinity of $\tilde{\omega}_{\mathrm{il}}$ is represented by different expressions for frequencies below and above $\tilde{\omega}_{\mathrm{il}}$, respectively,

$$\lambda = \frac{1}{2l_0}\left(\frac{1}{4pl_0}\right)^{1/3}\left[1 + \frac{12}{d}\frac{(\gamma l_0)^{1/2}}{(4l_0 p)^{1/6}}(\tilde{\omega}_{\mathrm{il}}^2 - \omega^2)^{1/2}\right],$$

$$\lambda = \frac{1}{2l_0}\left(\frac{1}{4pl_0}\right)^{1/3}\left[1 - \frac{12}{d}\frac{\gamma l_0}{(4l_0 p)^{1/3}}(\omega^2 - \tilde{\omega}_{\mathrm{il}}^2)\right], \tag{51}$$

reflecting a discontinuity of its frequency derivative at the spectrum boundary. The LE itself is, of course, continuous at $\tilde{\omega}_{\mathrm{il}}$, giving rise to the localization length $l = 2l_0(4pl_0)^{1/3}$ at the edge of the band. It is interesting to compare this expression with the localization length at the center of the impurity band, Eq. (41). They both grow with the concentration, but the latter one is much smaller and demonstrates slower fractional concentration dependence.

At the upper impurity band edge Ω_1 the integral DOS, $N(\omega)$, diverges, causing much stronger singularity in the differential DOS than at the lower boundary ω_{il}:

$$\rho(\omega) = \frac{d\omega p^{1/2}}{\pi c(\Omega_1^2 - \omega^2)^{3/2}}, \tag{52}$$

which is typical for the DOS in the vicinity of resonance frequencies. Comparing this expression with a similar formula for a pure chain, one can again interpret this result as a renormalization of the velocity parameter c by the concentration of impurities, which is different from that presented by Eq. (50) by a numerical coefficient only.

The last spectrum boundary is the bottom of the upper polariton branch Ω_L. The spectrum in the vicinity of this frequency exists in the absence of the impurities, which are responsible for two effects in this region. First, they move the boundary from Ω_L to higher frequencies [Eq. (46)]; second, they increase the effective mass of the upper polariton branch, such that the differential DOS in the frequency region above $\tilde{\omega}_{\mathrm{up}}^2$ becomes

$$\rho(\omega) = \frac{1}{\pi dc}\frac{\omega}{[\omega^2 - \tilde{\omega}_{\mathrm{up}}^2(p)]^{1/2}} \times \left\{1 + \frac{p}{2}\left[\frac{d^2(\Omega_1^2 - \Omega_0^2)}{d^2 - (\Omega_1^2 - \Omega_0^2)}\right]^2\right\}. \tag{53}$$

This expression can also be interpreted as a renormalization of the speed of light c.

4. CONCLUSION

In the paper we have presented a detailed study of an impurity-induced band of excitations, which arise in the gap between lower and upper polariton branches of a linear chain with dipole active atoms. We have also studied impurity-induced effects on properties of the regular po-

lariton branches. The method of microcanonical ensemble in conjunction with the expansion in the parameter $l_{\mathrm{def}}/l_0 \ll 1$, where l_{def} is the average distance between the impurities and l_0 is the localization radius of a single local polariton state, produces a clear physical description of the excitations and shows excellent agreement with the results of numerical simulations. In the zero order of this expansion we recover the DOS and the dispersion law of excitations in the system with uniform continuously distributed impurities. Corrections to this solution describe effects owing to local fluctuations in the positions of impurities such as a finite localization length of the excitations, a renormalization of the spectral boundaries, and the effective mass of the excitations. Therefore the parameter l_{def}/l_0, can be considered as a measure of disorder in the system.

We found that the dispersion law of the impurity-band excitations at the lower-frequency spectral boundary resembles that of the upper regular polariton band, but with a significantly (by a factor of $p^{1/2} \ll 1$) reduced effective mass. At the higher-frequency edge of the band the wave number diverges in a manner similar to the regular lower polariton branch with a velocity parameter again reduced by the same factor. The group velocity of the excitations near the center of the band, as well as the localization length, is proportional to p. However, the latter demonstrates a parabolic frequency dependence with the curvature of the parabola falling off with an increase of the concentration as $1/p^2$. Excitations considered in this paper are drastically different from impurity-induced polaritons studied in Ref. 17. The authors of the latter paper considered excitations of an ordered chain of two-level atoms embedded in a polar 1D crystal. Most significantly, the effective mass of polaritons of Ref. 17 is negative at the long-wave boundary of the spectrum whereas our excitations have a positive effective mass in this region; concentration dependencies of the effective mass and the bandwidth also differ significantly.

The regular expansion in powers of the parameter l_{def}/l_0 produces diverging expressions at the boundaries of the zero-order spectrum. Allowing for fractional powers in the expansion, we obtained a finite regularized expression for the density of states and the localization length at the boundaries. It is interesting to note that renormalized DOS at the lower boundary of the impurity band differs from its initial form only by a numerical factor of 3, whereas the position of the boundary is shifted toward lower frequencies.

The considered model can be applied to two different experimental situations. First, it describes certain properties of excitations that could arise in 3D polar dielectrics with some special type of impurities. In this case an experimental significance of the results presented is affected by two factors: absorption that is due to a different kind of anharmonic processes, and the 1D nature of the considered model. Effects that were due to absorption were studied numerically with absorption introduced phenomenologically. We found that at low-enough temperatures the impurity-induced band survives the absorption and can be observed. As for the one dimensionality of our model, it is generally accepted (see for instance Ref. 8) that 1D models give a fair description of tunneling in the limit of small concentrations ($l_{\mathrm{def}}/l_0 \gg 1$). We deal with the opposite limit; however, our zero-order results could describe the dispersion law of excitations in the real 3D medium propagating in one specified direction (for example, the direction with the highest symmetry). Disorder in this case would lead, of course, to scattering and deviation from 1D geometry, but effects that are due to disorder are much weaker in three dimensions and would probably not inhibit an observation of a defect-induced transparency in the frequency region of a polariton gap. Besides, as we have mentioned before, viability of 1D models in describing dynamics of mixed crystals had been tested by many studies in the past.[25]

Another type of experimental situation relevant to the presented calculations is reflectance and luminescent studies of multiple-quantum-well structures with a large number of wells. Such studies have been carried out recently in Ref. 32, where reflectance and luminescent spectra of structures with up to 100 QW's were studied. Introducing into such a structure a single QW with exciton resonance frequency inside the forbidden gap of the host structure must give rise both to a local polariton state[33] and to strong transmission resonance and a narrow luminescent line at the frequency of the local state. The quantitative analysis of Refs. 23 and 24 and of the present paper can be directly applied to so-called short-period QW structures with periods much smaller than the electromagnetic wavelength. In the case of QW structures with periods compared with the wavelength, which currently attract a great deal of interest, some additional analysis of local state frequencies is required. This analysis is under way.

ACKNOWLEDGMENTS

We are pleased to acknowledge the valuable remarks of A. J. Sievers. We wish to thank S. Schwarz for reading and commenting on the manuscript. This work was supported by the National Science Foundation under grant DMR-9632789 and by a City University of New York collaborative grant.

REFERENCES

1. S. John, "Electromagnetic absorption in a disordered medium near a photon mobility edge," Phys. Rev. Lett. **53**, 2169–2172 (1984).
2. D. S. Wiersma, P. Bartolini, A. Lagendijk, and R. Righini, "Localization of light in a disordered medium," Nature **390**, 671–673 (1997).
3. E. Yablonovitch, "Inhibited spontaneous emission in solid-state physics and electronics," Phys. Rev. Lett. **58**, 2059–2062 (1987).
4. J. D. Joannopoulos, R. D. Meade, and J. N. Winn, *Photonic Crystals: Molding the Flow of Light* (Princeton University, Princeton, N.J., 1995).
5. S. John, "Strong localization of photons in certain disordered dielectric superlattices," Phys. Rev. Lett. **58**, 2486–2489 (1987).
6. I. M. Lifshitz, "Some problems of the dynamic theory of non-ideal crystal lattices," Nuovo Cimento **3**, 716–734 (1956).
7. I. M. Lifshitz and A. M. Kosevich, "The dynamics of a crystal lattice with defects," in *Lattice Dynamics* (Benjamin, New York, 1969), pp. 53–90.
8. I. M. Lifshitz and V. Ya. Kirpichnikov, "Tunnel transpar-

ency of disordered systems," Sov. Phys. JETP **50**, 499–511 (1979).
9. A. A. Maradudin, "Some effects of point defects on the vibrations of crystal Lattices," in *Lattice Dynamics* (Benjamin, New York, 1969), pp. 1–52.
10. A. A. Maradudin, E. W. Montroll, G. H. Weiss, and I. P. Ipatova, *Theory of Lattice Dynamics in the Harmonic Approximation*, 2nd ed. (Academic, New York, 1971).
11. B. I. Schklovskii and A. L. Efros, *Electron Properties of Doped Semiconductors* (Springer, New York, 1984).
12. E. Yablonovitch, "Inhibited spontaneous emission in solid-state physics and electronics," Phys. Rev. Lett. **58**, 2059–2062 (1987); S. John and T. Quang, "Spontaneous emission near the edge of a photonic band gap," Phys. Rev. A **50**, 1764–1769 (1994).
13. E. Yablonovitch, T. J. Gmitter, R. D. Meade, A. M. Rappe, K. D. Brommer, and J. D. Joannopoulos, "Donor and acceptor modes in photonic band structure," Phys. Rev. Lett. **67**, 3380–3383 (1991).
14. R. D. Meade, K. D. Brommer, A. M. Rappe, and J. D. Joannopoulos, "Photonic bound states in periodic dielectric materials," Phys. Rev. B **44**, 13772–13774 (1991).
15. V. I. Rupasov and M. Singh, "Quantum gap solitons and soliton pinning in dispersive medium and photonic-band-gap materials: Bethe-ansatz solution," Phys. Rev. A **54**, 3614–3625 (1996); "Two-atom problem and polariton-impurity band in dispersive media and photonic-band-gap materials," Phys. Rev. A **56**, 898–904 (1997)
16. S. John and J. Wang, "Quantum electrodynamics near a photonic band gap: photon bound states and dressed atoms," Phys. Rev. Lett. **64**, 2418–2421 (1990); "Quantum optics of localized light in a photonic band gap," Phys. Rev. B **43**, 12772–12789 (1991)
17. M. R. Singh and W. Lau, "Polariton effective mass and spectral density in III–IV semiconductors doped with an ordered chain of identical two-level atoms," Phys. Status Solidi A **203**, 401–410 (1997).
18. A. A. Lisyansky and L. I. Deych, "Localization of polaritons by impurities," Bull. Am. Phys. Soc. **42**, 203–204 (1997); L. I. Deych and A. A. Lisyansky, "Local polariton states in polar crystals with impurities," Phys. Lett. A **240**, 329–333 (1998).
19. V. S. Podolsky, L. I. Deych, and A. A. Lisyansky, "Local polariton states in impure ionic crystals," Phys. Rev. B **57**, 5168–5176 (1998).
20. V. M. Shalaev, R. Botet, and A. V. Butenko, "Localization of collective dipole excitations on fractals," Phys. Rev. B **48**, 6662–6664 (1993); S. I. Bozhevolnyi, V. A. Markel, V. Coello, W. Kim, and V. Shalaev, "Direct observation of localized dipolar excitations on rough nanostructured surfaces," Phys. Rev. B **58**, 11441–11448 (1998).
21. M. I. Stockman, L. N. Pandey, L. S. Muratov, and T. F. George, "Optical absorption and localization of eigenmodes in disordered clusters," Phys. Rev. B **51**, 185–195 (1995); M. I. Stockman, L. N. Pandey, and T. F. George, "Inhomogeneous localization of polar eigenmodes in fractals," Phys. Rev. B **53**, 2183–2186 (1996); M. I. Stockman, "Femtosecond optical responses of disordered clusters, composites, and rough surfaces: 'the ninth wave' effect," Phys. Rev. Lett. **84**, 1011–1014 (2000).
22. L. I. Deych and A. A. Lisyansky, "Resonance tunneling of polaritons in 1-D chain with a single defect," Phys. Lett. A **243**, 156–162 (1998).
23. L. I. Deych, A. Yamilov, and A. A. Lisyansky, "Defect-induced resonant tunneling of electromagnetic waves through a polariton gap," Europhys. Lett. **46**, 534–539 (1999).
24. L. I. Deych, A. Yamilov, and A. A. Lisyansky, "Effects of resonant tunneling in electromagnetic wave propagation through a polariton gap," Phys. Rev. B **59**, 11339–11348 (1999).
25. D. W. Taylor, "Phonon response theory and the infrared and Raman experiments," in *Optical Properties of Mixed Crystals*, R. J. Elliott and I. P. Ipatova, eds. (North-Holland, Amsterdam, 1988), pp. 35–132.
26. D. S. Citrin, "Exciton radiative decay and polaritons in multiquantum wells: quantum-well-to-superlattice crossover," Solid State Commun. **89**, 139–143 (1994).
27. E. L. Ivchenko, A. I. Nesvizhskii, and S. Jorda, "Bragg reflection of light from quantum-well structures," Phys. Solid State **36**, 1156–1161 (1994).
28. L. C. Andreani, "Polaritons in multiple quantum wells," Phys. Status Solidi B **188**, 29–42 (1995).
29. T. Stroucken, A. Knorr, P. Thomas, and S. W. Koch, "Coherent dynamics of radiatively coupled quantum-well excitons," Phys. Rev. B **53**, 2026–2033 (1996).
30. Y. Merle, D. Aubigné, A. Waseila, H. Mariette, and T. Dietl, "Polariton effects in multiple-quantum-well structures of $CdTe/Cd_{1-x}Zn_xTe$," Phys. Rev. B **54**, 14003–14011 (1996).
31. M. Hübner, J. Kuhl, T. Stroucken, A. Knorr, S. W. Koch, R. Hey, and K. Ploog, "Collective effects of excitons in multiple-quantum-well Bragg and anti-Bragg structures," Phys. Rev. Lett. **76**, 4199–4202 (1996).
32. M. Hübner, J. P. Prineas, C. Ell, P. Brick, E. S. Lee, G. Khitrova, H. M. Gibbs, and S. W. Koch, "Optical lattices achieved by excitons in periodic quantum well structures," Phys. Rev. Lett. **83**, 2841–2844 (1999).
33. D. S. Citrin, "Waveguiding without a waveguide: local-mode exciton polaritons in multiple quantum wells," Appl. Phys. Lett. **66**, 994–996 (1995).
34. A. Dereux, J.-P. Vigneron, P. Lambin, and A. Lucas, "Polaritons in semiconductor multilayered materials," Phys. Rev. B **38**, 5438–5452 (1988).
35. M. L. H. Lahlaouti, A. Akjouj, B. Djafari-Rouhani, and L. Dobrzynski, "Resonant and localized electromagnetic modes in finite superlattices," Phys. Rev. B **61**, 2059–2064 (2000).
36. D. Citrin, "Coherent transport of excitons in quantum-dot chains: role of retardation," Opt. Lett. **20**, 901–903 (1995).
37. J. M. Deutsch and G. Paladin, "Product of random matrices in a microcanonical ensemble," Phys. Rev. Lett. **62**, 695–699 (1989).
38. I. M. Lifshitz, S. A. Gredeskul, and L. A. Pastur, *Introduction to the Theory of Disordered Systems* (Wiley, New York, 1988).
39. D. J. Thouless, "A relation between the density of states and range of localization for one dimensional random system," J. Phys. C **5**, 77–81 (1972).